Indonesian Journal of Electrical Engineering and Computer Science
Vol. 20, No. 3, December 2020, pp. 1576~1583
ISSN: 2502-4752, DOI: 10.11591/ijeecs.v20.i3.pp1576-1583

Near-lossless image compression using an improved edge adaptive hierarchical interpolation

Yenewondim Biadgie
Department of software, Ajou Univesity, Republic of Korea

Article Info

Article history:

Received Jun 1, 2020
Revised Jul 23, 2020
Accepted Aug 15, 2020

Keywords:

Hierarchical encoding
Lossless image compression
Lossy image compression
Near-lossless compression
Progressive Transmission

ABSTRACT

Lossy image compression of medical images is required to store efficiently a huge amount of medical data on a remote storage device and to reduce transmission time of the image across a low-bandwidth communication. On the other hand, lossless compression of medical images is recommended because the loss of minor information leads to wrong medical diagnosis results that affects the life of patinets. To compromise the conflicting requirements of lossy and lossless image compression methods, a near-lossless image compression method is proposed.In the previous work, an edge adaptive hierarchical interpolation (EAHINT) algorithm was proposed for progressive lossless image compression. In this paper, EAHINT algorithm was enhanced for scalable near-lossless image compression. The proposed interpolation algorithm has three linear components, namely, one-directional, multi-directional and non-directional linear interpolators. The EAHINT algorithm swiches adaptively among the three linear interpolators based on the strength of the edge in a local context of the current pixel being predicted. The strength of the edge in local window was estimated using the variance of the pixels in the local window. Although the actual predictors are still linear functions, the switching mechanism tried to deal with non-linear structures like edges. Simulation results demonstrate that the improved interpolation algorithm has better compression ratio over the original EAHINT algorithm and JPEG-Ls image compression standard.

Corresponding Author:

Yenewondim Biadgie,
Department of sofware and Computer Engineering,
Ajou Univesity,
Suwon, 16499 – Republic of Korea.
Email: wondim@ajou.ac.kr

1. INTRODUCTION

In image compression, high priority has been given for compression ratio criteria. In line with this, the compression performance of a multi-resolution (hierarchical) image compression method is lower than the compression performance of a single resolution(non-hierachical) image compression method. As a result of this, multi-resolution form of image compression has not been very popular for lossless applications [1-3]. However, progressive image transmission mode of muti-resolution image encoding scheme is required when the size of the image data over a slow link is very large. Pyramid algorithms such as hierarchical interpolation (HINT) [4], interleaved hierarchical interpolation (IHINT) [5] and new interleaved hierarchical interpolation (NIHINT) [6] have been shown to be superior among hierarchical form of lossless image compression techniques in medical imaging.

In these pyramid algorithms, the predictor coefficients are constant for all input images as well as for all levels of the pyramid in the same input image. Since these algorithms are based on space-invariance model, they fail to capture the fast changing statistics around edges. To address this problem, edge adaptive hierarchical interpolation (EAHINT) scheme was developed [7, 8]. In this paper, EAHINT is improved by

improving the down sampling method of the image. Experimental results demonstrate that the new image down sampling method improves the compression ratio of interpolation errors of the images over the original EAHINT algorithm and JPEG-LS image compression standard.

The rest of the paper is organized as follows. In section 2, a review of lossy, lossless and near-lossless mode of image compression algorithms is given. In section 3, an overview of the improved edge adaptive hierarchical interpolation (I-EAHINT) for progressive near-lossless image encoding is described. In section 4, each components of the I-EAHINT scheme is described in detail. The experimental results are presented in section 5. Finally, the conclusions are derived in section 6.

2. REVIEW OF LOSSY, LOSSLESS AND NEAR-LOSSLESS COMPRESSION METHODS

Spatially adaptive linear interpolation techniques have been proposed for lossy image compression by means of least-squares optimization [9-15]. They are effective for an arbitrary edge direction. However, finding the optimal coefficients is computationally very expensive because the least-squares covariance matrix is computed for each pixel from its large size local window. Hence, the use of these complex algorithms is limited to develop fast and real-time image transmission systems. To address this problem, a number of simple pyramid data structures have been developed for lossless multi-resolution image coding scheme, namely, the hierarchical INTerpolation (HINT) [4], the interleaved hierarchical INTerpolation (IHINT) [5], the new interleaved hierarchical INTerpolation (NIHINT) [6], edge adaptive hierarchical INTerpolation (EAHINT) [7] and other hierarchical image compression methods [16, 17]. The weakness of HINT, IHNIT and NIHINT prediction algorithms is explained in detail in [7].

Generally, these interpolative algorithms do not use techniques to identify the directions of strong intensity correlations near the target pixel so as to exploit the directional correlations among neighboring pixels. As a result of this, interpolation errors along sharp edges are large and cannot be encoded efficiently by entropy coders. To address the weakness of these interpolation methods, Edge Adaptive Hierarchical INTerpolation (EAHINT) was developed [7]. Based on the local variance of the casual context of the current pixel, the EAHINT algorithm has three statistical decision rules to classify the strength of the local edge into strong, weak, or medium.

By definition, in near-lossless image compression, the value of any pixel of a decompressed image is not changed in magnitude by more than σ-gray level value when it is compared with the original gray level value. Assume a gray level image with R number of rows and C number of columns is denoted by a 2-dimentional array of integer values $I(i,j)$, where $0 \le i < R$ and $0 \le j < C$. Assume that the decompressed version of the image I is denoted by $\tilde{I}(i,j)$. Based on these two assumptions, the purpose of σ-level near-lossless image compression is to obtain a decompressed (approximation) image $\tilde{I}(i,j)$ which satisfies the following equation.

$$\|x\|_{\infty} = MAX\left|I(i,j) - \tilde{I}(i,j)\right| \le \sigma, \quad (1)$$

where σ is the level of error tolerance. In this paper, the value of σ is 1. Hence, near-lossless image compression has been proposed as trade-off between low compression ratio of lossless image compression algorithm and high distortion of lossy image compression algorithm [18-23].

3. OVERVIEW OF THE IMPROVED EAHINT FOR NEAR-LOSSLESS COMPRESSION

The improved EAHINT algorithm and the original EAHINT are different significantly in the information of the low sub-band component of the hierarchical represenation of the image. However, both methods use similar prediction context to interpolate the current pixe. In both methods, the value of the current pixel *c* is interpolated by determining the strength and direction of the local edge as shown in Figure 1.

P_1	P_2	P_3
P_4	**C**	P_5
P_6	P_7	P_8

Figure 1. A 3x3 rectangular window of neighboring pixels to predict the current pixel **C**

The variance (σ^2) of the causal neighbors of the current pixel c is used to estimate the activity level of the prediction context. Using the value of the local variance, the local area can be classified as an edge area or a smooth area. Hence, the predictor switches between a non-directional linear interpolator for a smooth area and a one-directional interpolator for an edge area. A multi-directional interpolator is also used as a compromise between the two extreme edge strengths. Based on Figure 1, the pseudo code of the main components of the EAHINT algorthim is given as follows.

The Pseudo Code of EAHINT Algorithm to Interpolate Central Pixel C

1. Let **P** = (P_1, P_2, P_3, P_4, P_6, P_7, P_8) be a local vector from a 3x3 local window as shown in Figure 1.
2. Set two threshold values : T_1 and T_2
3. Calculate variance δ^2 of the local window **(P)**
4. **if** ($\delta^2 > T_2$)
5. {
6. Compute mean $\bar{x}$ of local window**(P)**
7. **if** $P_i \leq \bar{x}$
8. Assign P_i to Group 1, where i = 1, 2, 3, 4 ,6, 7, 8, and 9
9. e**lse**
10. Assign P_i to Group 2, where i = 1, 2, 3, 4, 6, 7, 8, and 9
11. Compute δ^2_1 and δ^2_2 for each group
12. **if** ($\delta^2 > \delta^2_1 + \delta^2_2$)
    Go to line 19.
13. **else**
    Go to line 20.
14. }
15. **else if** ($T_1 < \delta^2 \leq T_2$)
16. Go to line 20.
17. **else**
18. Go to line 21.
19. One-Directional Linear Interpolator(P) as shown in [7]
20. Multi-directional Adaptive Weighing Linear Interpolator (P) as shown in [7]
21. Non-directional Static Weighting Linear Interpolator (P) as shown in [7].

Since the weight along one particular direction is dominant in the presence of a strong edge, interpolation is performed only along that particular direction. Since the weights are almost equivalent in the presence of weak edges (smooth regions), static weighting linear interpolation is used. For edges with medium strength, multi-directional adaptive weighing linear interpolator is used as a compromise between the two extreme types of edges. The formation of the low sub-band image using an improved image down sampling method is described in detail in the following section.

4. DETAILED DESCRIPTION OF IMPROVED EAHINT ALGORITHM

Assume the original image I is represented as a two dimensional array I $[R, C]$ where R is the number of rows and C is the number of columns of the original image I. The existing EAHINT algorithm for progressive lossless image compression is improved by generating low subband component of the original image using new image down sampling method. Both algorithms scan the original image three times to encode and transmit the image progressively. Figure 2 and Figure 3 shows a 3x3 shaded region as a casual context to interpolate the central pixel in the first three passes of the original EAHINT algorithm and its improved version, respectively. The difference between the original EAHINT algorithm and the improved EAHINT algorithm is described in detail in the following three sub-sections.

4.1. Formation and Extrapolation of a Low Sub-band Image

In the first pass of the original EAHINT algorithm [7], the low subband of an image is generated by simply sampling even-row and even-column indices $I(2i, 2j)$ from the original image I as shown in Figure 2(a). These pixels can be denoted by $L_1(i, j) = I(2i, 2j)$, where $0 \leq i < R/2$ and $0 \leq j < C/2$. The dimension of this sub-sampled image is I $[R/2, C/2]$.The subscript to L determine the stage of the scan of the original image. By using several scanning stages of the original image, a hierarchical pyramid data structure can be generated. However, in this paper, the input image is scanned three times to generate two hierchical resolutions of the original image.

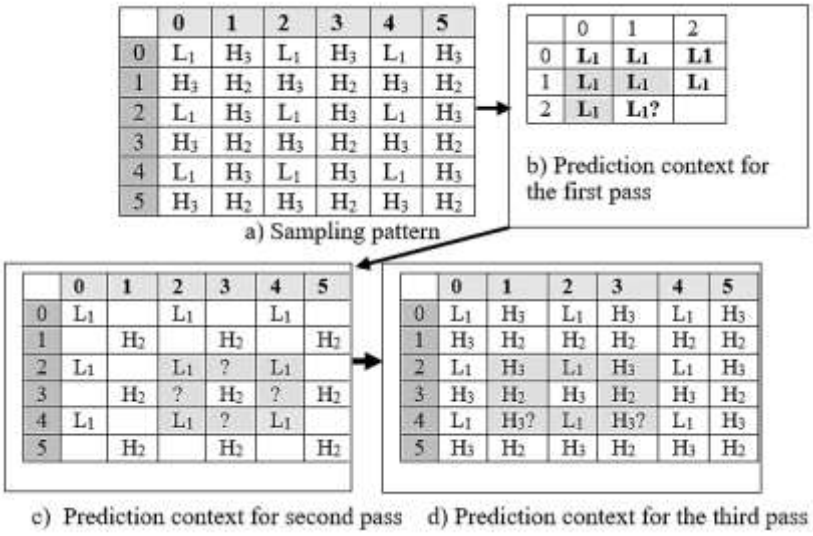

Figure 2. Hierarchical decomposition of an image into two layers by passing the image three times using the original EAHINT algorithm

In the original EAHINT algorithm, there is no low-pass filtering operation before image down sampling. Hence, to minimize the impact of low-pass filtering on the compression efficiency, the improved EAHINT algorithm creates the low subband (L) component of the original image by taking the average of a pair of adjacent diagonal pixels as shown in Figure 3. The pixels in the low subband image are created using the following equation [24].

$$L_1[i,j] = \frac{I(2i,2j)+I(2i+1,2j+1)}{2} = \frac{S[i,j]}{2} \quad (2)$$

where $s[i,j]$ is the sum of the two diagonal pixels, $0 \le i < R/2$ and $0 \le j < C/2$. Moreover, as the number hierarchical level K increases, the compression performance of the algorithm decreases due to the accumulated aliasing effect of high frequency subbands. Due to this reason, $K = 1$ is used in this paper.

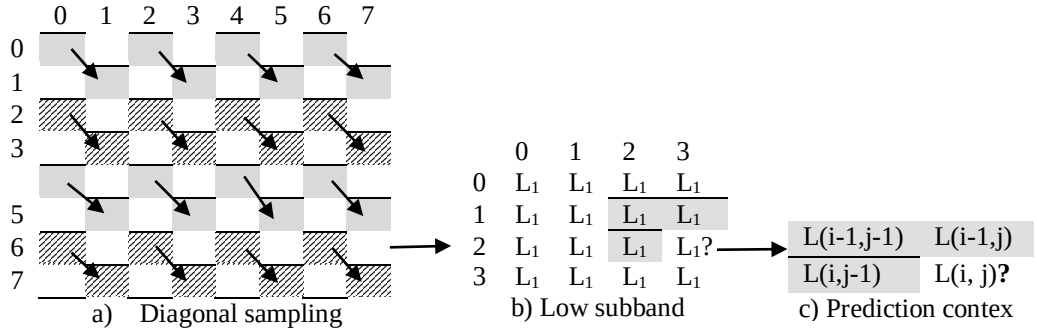

Figure 3. The formation and prediction context of low subband pixels L_1 in the first pass of improved EAHINT algoritm from a pair of adjacent diagonal pixels and their prediction casual context

As shown in Figure 3(c), any pixel in low subband image $L_i(i,j)$ is encoded sequentially by predicting the current pixel from its three-neighboring pixels using the median edge detector (MED) algorithm of JPEG-LS standard [25]. Since a pair of adjacent diagonal pixels are highly correlated in the original image, this correlation carries over to the low subband image. This approach increases the correlation among neighbouring pixels at the earlier scanning stage of the hierarchical coding [24]. This, in turn, makes the pixels to be compressed very well at the earlier scanning stages of the image.

From equation (2), the value of $S[i,j]$ can be even or odd. If the value of $S(i,j)$ is even, there is no truncation error in the creation of the pixel $L_1(i,j)$ when $S(i,j)$ is divided by 2. However, if the value of $S(i,j)$ is odd, there is a truncation error in the creation of the pixel $L_1(i,j)$ when $S(i,j)$ is divided by 2. This implies that 1-bit is lost among 8-bits of the original image due to truncation error. Hence, according to the definition of near-lossless image compression, the value of σ is 1 ($\sigma = 1$). Due to this reason, the improved EAHINT algorithm can be called near-lossless hierarchical image compression. Note that when both $I(2i,2j)$ and $I(2i+1,2j+1)$ diagonal pixels are even, their sum $S(i,i)$ is even. Moreover, when both $I(2i,2j)$ and $I(2i+1,2j+1)$ diagonal pixels are odd, their sum $S(i,j)$ is even. However, when one of diagonal pixels is odd and the other is even, their sum $S(i,j)$ is odd. If we consider the variable $S(i,j)$ as a uniform random variable, the probability of the random variable $S(i,j)$ to be even is $2/3$ and its probability to be odd is $1/3$. Mathematically, $P(S(i,j) = even) = 2/3$ and $P(S(i,j) = odd) = 1/3$. Hence, only one-third of the total number of pixels in a low subband image can have truncation error. However, for near-lossless image compression with $\sigma = 1$, each pixel has a truncation error of 1-bit. This implies that the improved EAHINT is not fully near-lossless image compression in comparison to the full near-lossless image compression with $\sigma = 1$.

4.2. Formation and Interpolation of High Subband (H_2) Pixels of an Image

In the second pass of the original EAHINT algorithm, high subband (H_2) pixels with odd-row and odd-column indices $I[2i+1, 2j+1]$ are encoded for $0 \leq i < R/2$ and $0 \leq j < C/2$ as shown in Figure 2(c). There are 8-connected neighboring pixels to interpolate the central pixel as shown in Figure 2(c). Among these 8-connected neighboring pixels, the 4-connected pixels are not available directly during the first pass as well as from the upper and left neighbours of the second pass itself and they are indicate by question mark (**?**) as shown in Figure 2(c). They are estimated from the average of a pair of vertical or horizontal adjacent pixels of the current pixel before computing the variance of the 3x3 local window as shown in [7].

On the other hand, in the second pass of the improved EAHINT algorithm, pixels with even-row and even-column indices $I(2i,2j)$ as well as pixels with odd-row and odd-column indices $I(2i+1,2j+1)$ are encoded at the same time by interleaving each other as shown in Figure 4, where H_2 denotes a pixel with index $I(2i,2j)$ and h_2 denotes the corresponding diagonal pixel with index $I(2i+1,2j+1)$. Practically, the encoder module does not encode h_2 pixels with index $I(2i+1,2j+1)$ because the decoder module can extract h_2 pixels from from equation(2) using the following equation.

$$h_2 = I(2i+1,2j+1) = 2L_1(i,j) - I(2i,2j) = 2L_1(i,j) - H_2 \quad (3)$$

where, $0 \leq i < R/2$ and $0 \leq j < C/2$. Similar to the original EAHINT, among the 8-connected casual predictor pixels of the central pixel, only the 4 pixels which are located at the diagonal direction of the central pixel are available directly. The remaining 4 pixels which are in the horizontal and vertical directions of the central pixel are not available directly. These missed pixels can be estimated by taking the average of its pair of adjacent pixels in the horizontal or vertical direction before computing the variance of local window.

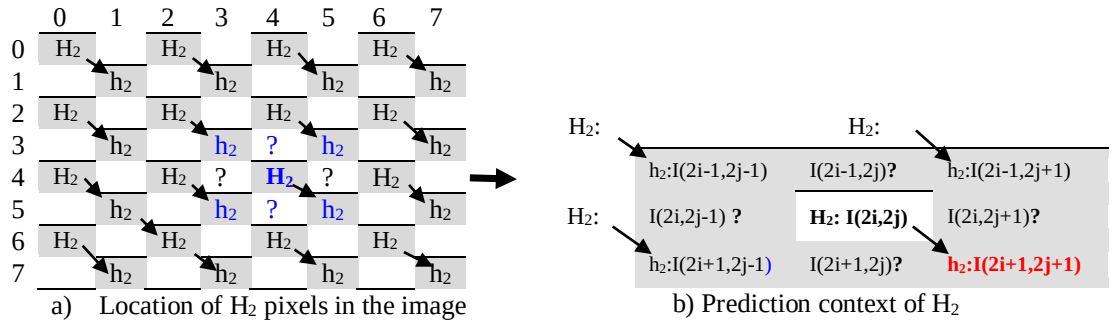

a) Location of H_2 pixels in the image b) Prediction context of H_2

Figure 4. A 3x3 casual prediction context for pixels in the second pass. a) Causal context of a pixel value at I (4, 4) as an example to illustrate context of H_2 pixels. b) Casual context of any H_2 and d h_2 pixel types type, where H_2 = I (2i, 2j) and h_2 = I (2i+1, 2j+1). Note that the h_2 pixels with red color in the improved EAHINT algoritm is different from the value of H_2 pixel types in the original EAHINT algorithm. In Figure 4(b), the h_2 pixels represent the value in low subband image. In other words, the value of h_2 pixels cannot be extracted by decoder because the decoder did not know the current central H_2 pixel, where H_2 = I (2i, 2j).

4.3. Formation and Interpolation of High Subband (H_3) Pixels of an Image

In the third pass of the original EAHINT algorithm, high subband (H_3) pixels with even-row and odd-column indices $I[2i, 2j+1]$ as well as odd-row and even-column indices $I[2i+1, 2j]$ are encoded by interlacing each other as shown in Figure 2(d). To predict pixels with index $I[2i, 2j+1]$ or $I(2i+1, 2j)$, among 8-connected neighbouring pixels, only 2 neighbouring pixels are not available directly to the central pixel. These neigbouring pixels are not available from the first pass, second pass as well as from the upper and left neighbours of the third pass itself. These two pixels can be computed from its four available pixels as shown in [7]. Similar to the original EAHINT algorithm, in the third pass of the improved EAHINT algorithm, high subband (H_3) pixels with even-row and odd-column indices $I[2i, 2j+1]$ as well as odd-row and even-column indices $I[2i+1, 2j]$ are encoded by interlacing each other as shown in Figure 5. Pixels with index $I[2i, 2j+1]$ or $I(2i+1, 2j)$ are predicted similar to the pixels in the original EAHINT algorithm.

	0	1	2	3	4	5
0	H_2	H_3	H_2	H_3	H_2	H_3
1	H_3	h_2	H_3	h_2	H_3	h_2
2	H_2	H_3	H_2	H_3	H_2	H_3
3	H_3	h_2	H_3?	h_2	H_3?	h_2
4	H_2	H_3	H_2	H_3	H_2	H_3
5	H_3	h_2	H_3	h_2	H_3	h_2

a) Location of H_2 pixels in the image

	H_3:I(2i-1,2j)	h_2:I(2i-1,2j+1)	H_3:I(2i-1,2j+2)	
	H_2:I(2i, 2j)	**H_3: I(2i, 2j+1)?**	H_2:I(2i, 2j+2)	
h_2:(2i+1,2j-1)	H_3:I(2i+1,2j) **?**	h_2:I(2i+1,2j+1)	H_3: I(2i+1,2j+2)?	h_2: I(2i+1,2j+3)
	H_2: I(2i+2,2j)		H_2: (2i+2,2j+2)	

b) Prediction context of H_2

Figure 5. A 3x3 casual prediction in the third pass; a) causal context of the pixel I (2, 3) as an example of H_3 pixels (high-band pixels). b) Causal context of any H_3 pixel types, H_3 = I (2i, 2j+1) or H_3 = (2i+1, 2j)

5. RESULTS AND DISCUSSION

In this section, we evaluate the performance of the improved EAHINT (I-EAHINT) algorithm for progressive near-lossless image compression in comparison to the original algorithm EAHNT (O-EAHINT) for progressive lossless image compression. It is also compared with the JPEG-LS standard [24]. Six common standard test images with 8 bits per pixel and size of 512x512 are used in our experiments as shown in Figure 6. The comparison of the compression ratio of the improved EAHINT algorithm with the original EAHINT and the JPEG-LS is presented in Table 1. The compression ratio is obtained by dividing the total number of bytes of the input image before compression by the total number of bytes after compression. Therefore, the more the compression ratio, the better the performance of the encoder algorithm. For all test images, the improved EAHINT method performs better than the other two methods. On average, the improved EAHINT algorithm improves the compression ratio of the original EAHINT algorithm by 2.73%. It also improves the compression ratio of JPEG-LS algorithm by 1.75%. The performance of the improved EAHINT algorithms increases as the number of layers of the herachical image represenation increases from two layers into three more layers. Moreover, the performance of the improved EAHINT algorithms increases by adding context adaptive error correction model as shown in [8].

The compression ratio of the improved EAHINT method is better than the compression ratio of the other two methods because of the following two reasons. The first reason is that in the first pass of the original EAHINT algorithm, low subband pixels are far apart by one pixel with each other due to image down sampling without using low-pass filtering as shown in Figure 2(a). This implies that since image down sampling in an edge area introduces uncertainty about the direction and exact location of the edge in the original image, a large interpolation error will be created if the interpolation is done across sharp edges instead of doing

along the direction of the sharp edge. The second reason for the better performance of the improved EAHINT algorithm is the presence of data redundancy in the low subband image. Since a pair of adjacent diagonal pixels are highly correlated in the original image, the accuracy of the prediction of the current pixel increases. This implies that the subband image can be compressed easily.

Baboon Boat Lena Pepper Sailboat Women

Figure 6. Images used for the experimental evaluation of the improved EAHINT Algorithm

Table 1. Comparision of the compression ratio of the improved EAHINT algorithm with the original EAHINT algorithm and JPEG-LS standard

Image	EAHINT	JPEG-LS	IEAHINT
Baboon	1.32	1.33	1.34
Boat	1.65	1.67	1.68
Lena	1.90	1.89	1.95
Pepper	1.76	1.78	1.80
sailboat	1.58	1.61	1.61
women	1.95	1.94	2.01
Average	**1.69**	**1.70**	**1.73**

6. CONCLUSION

In this paper, a near-lossless progressive image compression is developed by improving the low subband image formation method of the original EAHINT algorithm. The low band image formation is improved by using a diagonal of two adjacent pixels as a simple form of a low-pass filter. This operation increases the correlation among the neighbouring pixels in the low subband image. This, in turn, makes the prediction errors in the low subband images to be encoded efficiently. The improved algorithm uses the correlation among neighbouring pixels to extract higher order local image structures such as texture, edge and corner in a better way by using circular context. Since two-third of the total number of pixels in the low-band image have no truncation error, the improved EAHINT algorithm is not fully near-lossless. Hence, the improved algorithm balances the trade-off between fully lossless and fully near-lossless for medical image applications.

To model the non-linearity of the image structure, a nonlinear method for hierarchical image interpolation is used. Based on the strength of local edge, the interpolator switches among three linear interpolators. Since only the causal contexts are used in the encoder, no additional side information needs to be transmitted to the decoder and the decoder also has the same interpolator as the encoder.

REFERENCES

[1] A. J. Penrose, "Extending Lossless Image Compression," *Technical Report UCAM-CL-TR-526*, University of Cambridge, Dec. 2001.
[2] M. Goldberg and L. Wang, "Comparative Performance of Pyramid Data Structures for Progressive Image Transmission," *IEEE Transactions on Communications*, vol. 39, no. 4, pp. 540-548, Apr. 1991.
[3] Y.-K. Chee, "Survey of Progressive Image Transmission Methods," *International Journal of Imaging Systems and Technology*, vol. 10, no. 1, pp. 3-19, 1999.
[4] P. Roos, et al., " Reversible Intraframe Compression of Medical Images," *IEEE Transactions on Medical Imaging*, vol. 7, no. 4, pp. 328-336, Dec. 1988.
[5] A. Abrardo, et al., "Encoding Interleaved Hierarchical Interpolation for Lossless Image Compression," *Signal Processing*, vol. 56, no. 3, pp. 321-328, Feb. 1997.
[6] B. Zeng, et al., "New Interleaved Hierarchical Interpolation with Median Based Interpolators for Progressive Image Transmission," *Signal Processing*, vol. 81, no. 2, pp. 431-438, Feb. 2001.
[7] Y. Biadgie, et al., "Edge Adaptive Hierarchical Interpolation for Lossless and Progressive Image Transmission," *KSII Transactions on Internet and Information Systems*, vol. 5, no. 5, pp. 2068-2086, Nov. 2011.

[8] Biadgie, et al., " Multi-resolution Lossless Image Compression for Progressive Transmission and Multiple Decoding Using an Enhanced Edge Adaptive Hierarchical Interpolation," *KSII Transactions on Internet and Information Systems*, vol. 11, no. 12, pp. 6017-6037, Dec. 2017.
[9] X. Li and M. Orchard,"New Edge-directed Interpolation," *IEEE Transactions on Image Processing*, vol. 10, no. 10, pp. 1521-1527, Oct. 2001.
[10] N. Asuni and A. Giachetti, "Accuracy Improvements and Artifacts Removal in Edge Based Image Interpolation," *In Proc. of 3rd International Conference on Computer Vision Theory and Applications*, Vol. 1, pp. 58-65, Jan. 2008.
[11] X. Zhang and X. Wu, "Image Interpolation by Adaptive 2-D Autoregressive Modeling and Soft-decision Estimation," *IEEE Transactions on Image Processing*, vol. 17, no. 6, pp. 887-896, Jun. 2008.
[12] W. Tam, et al., "A Modified Edge Directed Interpolation for Images," *in Proc. of 17th European Signal Processing Conference*, pp. 283-287, Aug. 2009.
[13] K. Hung and W. Siu, "Improved Image Interpolation Using Bilateral Filter for Weighted Least Square Estimation," *in Proc. of 17th IEEE Internal Conference on Image Processing*, pp. 3297-3300, Sep. 2010.
[14] L.-J. Kau and Y.-P. Lin, "Least Squares Based Switching Structure for Lossless Image Coding," *IEEE Transactions on Circuits and Systems I*, vol. 54, no. 7, pp. 1529-1541, Jul. 2007.
[15] M. Frucci, et al., "An Automatic Image Scaling up Algorithm," *Lecture Notes in Computer Science* , vol.7329, pp. 35–44, Jun. 2012.
[16] S. Kim and N. I. Cho, "Hierarchical Prediction and Context Adaptive Coding for Lossless Color Image Compression," *IEEE Transactions on Image Processing*, vol. 23, no. 1, pp. 445-449, Jan. 2014.
[17] P. S. Babu and S. Sathappan, "Efficient Lossless Image Compression Using Modified Hierarchical Forecast and Context Adaptive System," *Indian Journal of Science and Technology*, vol. 8, no. 34, pp. 1-6, Dec. 2015.
[18] J. Taquet and C. Labit, "Hierarchical Oriented Predictions for Resolution Scalable Lossless and Near-Lossless Compression of CT and MRI Biomedical Images," *IEEE Transactions on Image Processing*, vol. 21, no. 5, pp. 2641-2652, May, 2012.
[19] J. Taquet and C. Labit, "Near-lossless and Scalable Compression for Medical Imaging Using a New Adaptive Hierarchical Oriented Prediction," *2010 IEEE International Conference on Image Processing*, pp. 481-484, 2010.
[20] A. S. Mamatha and V. Singh, "Near Lossless Image Compression System," *2012 Asia Pacific Conference on Postgraduate Research in Microelectronics and Electronics*, pp. 35-41, 2012.
[21] M. Domanski and K. Rakowski, "Lossless and near-lossless image compression with color transformations," *Proceedings 2001 International Conference on Image Processing*, vol. 3, pp. 454-457, 2012.
[22] Xiaoying, et al., "Novel Near-Lossless Compression Algorithm for Medical Sequence Images with Adaptive Block-Based Spatial Prediction." *Journal of digital imaging*, vol. 29, no. 6, pp. 706-715, 2016.
[23] C. P. Devadoss and B. Sankaragomathi, " Near Lossless Medical Image Compression Using Block BWT–MTF and Hybrid Fractal Compression Techniques," *Cluster Computing*, vol. 22, no.5, pp. 12929–12937, 2019.
[24] X. Wu, "Lossless Compression of Continuous-tone Images via Context Selection, Quantization and Modeling," *IEEE Transactions on Image Processing*, vol. 6, no. 5, pp. 656-664, May 1997.
[25] M. Weinberger, et al., "The LOCO-I Lossless Image Compression Algorithm: Principles and Standardization into JPEG-LS," *IEEE Transactions on Image Processing*, vol. 9, no. 8, pp. 1309-1324, Aug. 2000.

BIOGRAPHIES OF AUTHOR

Yenewondim Biadgie received his B.S. degree in mathematics in 2000 from Bahirdar university and M.S. degree in Information Science in 2006 from AddisAbaba university, Ethiopia. He also received his Ph.D. in Computer Engineering in 2012 from Ajou University, South Korea. He is currently an assistant professor in the department software and somputer engineering, at Ajou University South Korea starting from September 1, 2015. His research interest includes image and video compression, computer vision, pattern recognition, data mining, machine learning and deep learning.